J Therm Anal Calorim (2017) 127:273–282
DOI 10.1007/s10973-016-5479-6

The estimation of thermal endurance for some heteropoly acidic catalysts from thermogravimetric decomposition data

Viorel Zoltan Sasca[1] · Orsina Verdeş[1] · Alexandru Popa[1]

Received: 1 November 2015 / Accepted: 11 April 2016 / Published online: 27 April 2016

Abstract The calculation of thermal endurance and the estimation of lifetime at certain temperatures based on thermogravimetric data for the tungstophosphoric acid, $H_3[PW_{12}O_{40}]\cdot H_2O$ (H_3PW) and its Cs acidic salts, pure or doped with Pd, were done. The calculation of catalyst's lifetime with high degree of confidence needs reliable values for activation energy. For this reason, the activation energy values were calculated with ASTM E 1641-04 "Standard Test Method for Decomposition Kinetics by Thermogravimetry" based on Flynn–Wall isoconversional method and with Friedman isoconversional method (differential model-free) for checking, because the last provides accurate values of activation energies compared with the integral model-free methods. The thermal decomposition of the H_3PW and some of its acidic Cs salts, pure or doped with Pd, occurs through the constitutional water release [the water formed of the protons and the oxygen from the $[PW_{12}O_{40}]^{3-}$] having as result the loss of acid sites (protons) and its catalytic activity diminution at the same time. The activation energies are reliable values for the conversion range of $5 \leq \alpha \leq 20$, but the value for $\alpha = 10$ % is recommended for the calculation of the lifetime. The estimation of lifetimes was done with ASTM E 1877-00 "Standard Practice for Calculating Thermal Endurance of Materials from Thermogravimetric Data" method. The estimated thermal life of the H_3PW and some of its acidic Cs salts pointed out a very good thermal endurance at temperatures below 573 K. The Pd doping decreases drastically the thermal endurance in all cases.

✉ Viorel Zoltan Sasca
viorelsasca@yahoo.co.uk

[1] Institute of Chemistry Timisoara, Romanian Academy, Bd. M. Viteazul 24, 300223 Timisoara, Romania

Keywords Tungstophosphoric acid · Cesium acidic tungstophosphates · Pd-doped heteropoly compounds · TG/DTG–DTA analysis · Activation energy · Isoconversional methods · Estimation of lifetime

Introduction

The calculation of thermal endurance and the estimation of the catalyst lifetime at certain temperatures are problems of high interest for the catalysts used in practice. For this purpose, a standard method based on thermogravimetric data is used. The calculation of catalyst's lifetime with high degree of confidence needs reliable values for activation energy. The model-free isoconversional methods represent a solution because the model-free analysis has as main advantages: the simplicity and the avoidance of the errors connected with the selection of a kinetic model [1].

Thus, the activation energy values calculated with respect to [2] that complies with such exactingness owing to the clear rules for: the sample shape, the experimental procedure and the calculation course based on Flynn–Wall isoconversional method (integral model-free) [3, 4]. Also, the activation energies were calculated with Friedman isoconversional method (differential model-free) for checking, because this provides more accurate values of activation energies compared with the integral model-free methods, which could give significant errors in the determination of the activation energy [1, 5, 6].

The tungstophosphoric acid, $H_3[PW_{12}O_{40}]\cdot H_2O$ (H_3PW) and its Cs acidic salts, pure or doped with Cu, Fe, Ni, Co, Pd, Pt and Rh, are the most known heteropoly compounds with application in catalysis [7–15]. The thermal decomposition of the H_3PW and some of its acidic Cs salts, pure or doped with Pd, occurs through the constitutive water

release that was formed of the protons and the oxygen from the $[PW_{12}O_{40}]^{3-}$ (Keggin unit—KU) having as result the loss of acid centers (protons) [16, 17]. Thus, deactivation of these catalysts could be the effect of protons loss or their blocking with strong chemisorbed species and carbonaceous deposit [18–21]. Therefore, in this work, the processes of constitutive water release of H_3PW and some of its acidic Cs salts, pure and doped with Pd, were studied in details and their activation energy was found with integral and differential isoconversional method. Based on the activation energy of constitutive water release, the lifetime was determined according to [22].

Materials and methods

Samples preparation

The cesium salts of $H_3[PW_{12}O_{40}]\cdot H_2O$ (H_3PW) were prepared by precipitation from an 0.1 M aqueous solution of the parent acid (Merck, p.a., $x = 13$ H_2O) adding drop by drop the required stoichiometric quantity of cesium nitrate as 1 M aqueous solution under stirring. The pH was kept under 1.5 during all syntheses. The suspensions were heated at 333–343 K under stirring until a paste was obtained. After, the samples were heated up to 523 K and were kept at this temperature 1 h, in air atmosphere, for nitrate anion total decomposition. Finally, the solid samples with the general formula $Cs_xH_{3-x}PW\cdot yH_2O$, where $x = 1$, 2 and 2.5, were obtained.

The $Cs_xH_{3-x}PW\cdot yH_2O$ doped with 0.25 Pd atom/KU was prepared as follows: The 0.1 M aqueous solution of $Pd(NO_3)_2$ was added into the $H_3PW\cdot 13H_2O$ solution of 0.1 M in the ratio 1:4 and after that, the required stoichiometric quantity of cesium nitrate as 1 M aqueous solution was poured drop by drop under stirring. The suspension of precipitate was heated at 333–343 K under stirring until a paste was obtained. The same procedure for drying and total decomposition of nitrate anion from samples was used.

The $H_3PW\cdot 6H_2O$ doped with 0.25 Pd atom/KU was obtained by heating at 333–343 K under stirring the 0.1 M aqueous solutions of $Pd(NO_3)_2$ and $H_3PW\cdot 13H_2O$ in the 1:4 ratio until a paste was formed. The samples were shaped up with the procedure described previously for drying and total decomposition of nitrate anion.

All synthesized compounds were characterized by FTIR, XRD and TG–DTA.

Fourier transform infrared (FTIR) analysis

The FTIR absorption spectra were recorded with a Jasco 430 spectrometer (spectral range 4000–400 cm^{-1} range, 256 scans and resolution 2 cm^{-1}) equipped with Ge/KBr window.

Before each measurement, the samples were kept in air until constant mass was reached and the samples were pelletized with KBr. The FTIR spectra were taken at room temperature in air atmosphere.

XRD analysis on powder

Powder X-ray diffraction patterns were obtained with a Bruker D8 Advance diffractometer using the CuK_α radiation (Ni filter on the diffracted beam, 40 kV and 40 mA) in a Bragg–Brentano geometry, with Soller and fixed slits and a NaI (Tl) scintillation detector, at angles within the range of $2\theta = 5°$–$60°$.

Thermal analysis

Thermal analysis was carried out using a TGA/SDTA 851-LF 1100 Mettler Toledo apparatus. The samples with mass of about 10–50 mg were placed in alumina crucibles of 150 μL. The measurements were performed in dynamic air atmosphere with the flow of 50 mL min^{-1}, by heating of samples with 10 K min^{-1} from 298 K up to 573 K, followed by an isothermal heating at 573 K for 60 min and a final heating with 2.5, 5, 7.5 and 10 K min^{-1} between 573 and 923 K with the purpose of the activation energies calculation.

The checking of the lifetime's prediction was carried out by the heating of samples of pure and Pd-doped H_3PW up to 623 K with 10 K min^{-1} and keeping these at 623 K for a time calculated to reach at 10 % conversion. The synthetic air with composition 80 % N_2 and 20 % O_2, free of CH compounds and nitrogen of 4.6 purity class was supplied from Linde.

Results and discussion

Structural characterization by FTIR and XRD

The synthesized heteropoly compounds—HPCs consist of KUs. The molecular structure of KU is considered as primary structure of HPCs. The IR spectra of KUs contain characteristic vibration bands like a true finger print: $-\nu_{as}P–O_i–W$, 1080–1081; $-\nu_{as}W–O_t$, 976–995; $\nu_{as}W–O_c–W$, 890–900; $-\nu_{as}W–O_e–W$, 800–810 cm^{-1} [23]. Weaker absorption bands due to δ (P–O–P) and ν_s (W–O–W) appeared at 596 and 525 cm^{-1}, respectively [24]. A large band 3000–3400 cm^{-1} is assigned to crystallization hydrogen-bonded water and to hydrogen-bond vibrations (hydrogen bonds formed between neighboring KUs). The other two bands in relation to water molecule vibration

(1710–1720 and 1618 cm^{-1}) are assigned to δ vibrations of protonated water (hydroxonium ions, H_3O^+ or $H_5O_2^+$)and to δ vibrations of nonprotonated water molecules , respectively [25, 26]. The registered FTIR spectra show the presence of the specific absorption bands for KUs in the H_3PW and its Cs salts and in the Pd-doped heteropoly compounds also, as can be observed from Fig. 1.

No significant differences between the FTIR spectra for H_3PW and its Cs salts and the spectra of the same heteropoly compounds doped with Pd were observed; therefore, it could be concluded that Pd does not affect significant the KU structure.

The FTIR spectra of samples heated at 873 K for 1 h show the complete disappearance of specific KU absorption bands for H_3PW and Pd-doped H_3PW and an increase of intensity for these bands with higher Cs/KU ratio (see Fig. 2). This means that only KUs of H_3PW are destroyed at this temperature and by the increasing of the Cs/KU ratio, the amount of KUs of Cs_3PW also increases, as it will be demonstrated further by the XRD and the thermal analyses.

The $H_3PW{\cdot}6H_2O$ and their Cs salts have crystal structure of cubic Pn3m symmetry according to literature [25–27]. The synthesized $H_3PW{\cdot}6H_2O$ and its Cs acidic salts and Pd-doped $H_3PW{\cdot}6H_2O$ and its Cs acidic salts show close X-ray diffraction spectra as can be seen in Fig. 3.

All HPCs containing Cs show larger widths of diffraction maxima and a shifting to higher angles at the same time with the increases in the content of Cs. However, the diffraction maxima from smaller angles of $2\theta = 10.3$ and 14.6 are reduced drastically for HPC containing Pd. Therefore, Cs^+ and Pd^{2+} exercise a significant influence over the secondary structure only, because IR characteristic bands remain practically unchanged.

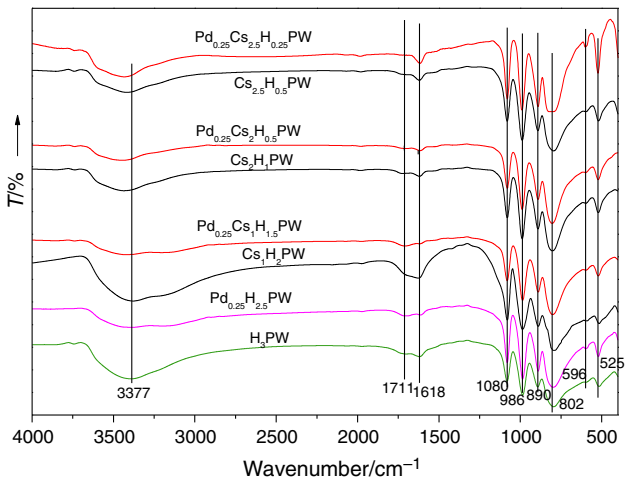

Fig. 1 FTIR spectra of H_3PW and $Cs_xH_{3-x}PW$, where $x = 1$, 2 and 2.5, and $PdH_{2.5}PW$ and $PdCs_xH_{2.5-x}PW$, where $x = 1$, 2 and 2.5

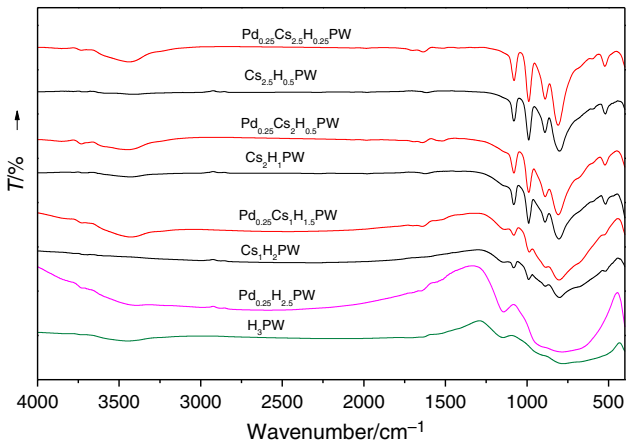

Fig. 2 FTIR spectra of the samples after calcination at 873 K, 1 h, in air atmosphere: H_3PW and $Cs_xH_{3-x}PW$, where $x = 1$, 2 and 2.5, and $PdH_{2.5}PW$ and $PdCs_xH_{2.5-x}PW$, where $x = 1$, 2 and 2.5

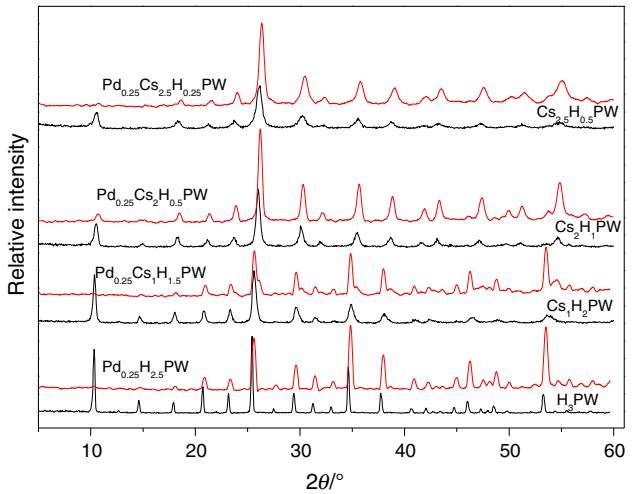

Fig. 3 X-ray diffraction patterns of H_3PW and $Cs_xH_{3-x}PW$, where $x = 1$, 2 and 2.5, and $PdH_{2.5}PW$ and $PdCs_xH_{2.5-x}PW$, where $x = 1$, 2 and 2.5

The analysis of the X-ray diffraction spectra from Fig. 3, by comparing with the spectra of Fig. 4, shows only the presence of the characteristic diffraction maxima for $H_3PW{\cdot}6H_2O$ and Cs_3PW. The files 00-050-304 for $H_3PW{\cdot}6H_2O$ and 00-050-1857 for Cs_3PW have found in the diffractometer's database.

The X-ray diffractograms of samples heated at 873 K are showed in Fig. 5. For identification of existent phases, these spectra have been compared with the most likely files of HPCs and oxides using the diffractometer's database and literature data.

The main lines of the X-ray files found in the spectra of Fig. 5 belong to WO_3 (00-004-5867 file plotted in Fig. 6) and Cs_3PW according to 00-050-1857 file. The results confirm the TG–DTA analyses and the IR investigations:

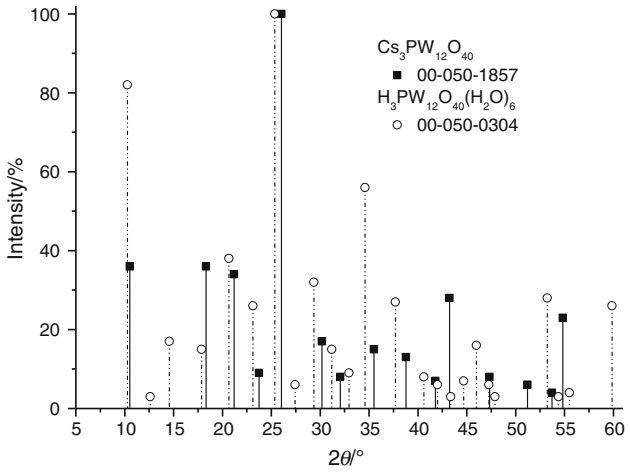

Fig. 4 X-ray diffraction lines for the main planes of reflections from $H_3PW{\cdot}6H_2O$ and Cs_3PW according to 00-050-304 file and 00-050-1857 file, respectively

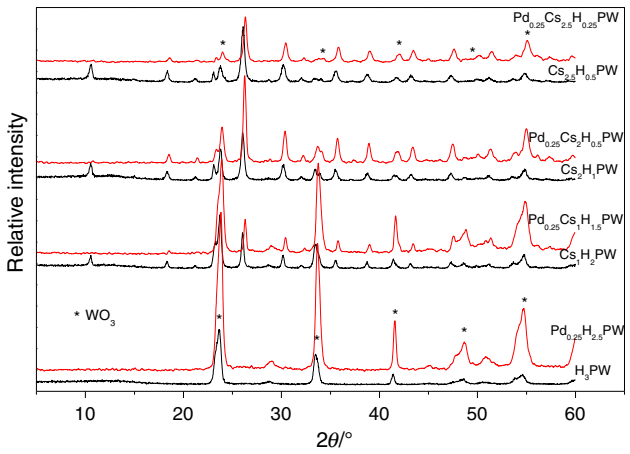

Fig. 5 X-ray diffraction patterns of H_3PW and $Cs_xH_{3-x}PW$, where $x = 1$, 2 and 2.5, and $PdH_{2.5}PW$ and $PdCs_xH_{2.5-x}PW$, where $x = 1$, 2 and 2.5, after calcination at 873 K, 1 h, in air atmosphere

the H_3PW was decomposed totally to corresponding oxides and the WO_3 was crystallized, because the H_3PW heated at 873 K gives a spectrum similar to the spectrum corresponding to tetragonal WO_3 [28, 29]. The tetragonal WO_3 is present also in the spectra of acidic salts as a result of its partial decomposition, because its main characteristic line (100) can be observed in these spectra. The intensities of this diffraction line decrease with respect to Cs/KU ratio increases. The main reflections lines of the Cs_3PW were observed, and their intensity increases for higher Cs/KU ratio. In the same time, the H_3PW's diffraction lines disappear practically.

WO_3 and PdO, both crystallized in tetragonal form, give close reflection lines, so PdO presence can be proved only by the comparison of the ratios between the heights for the

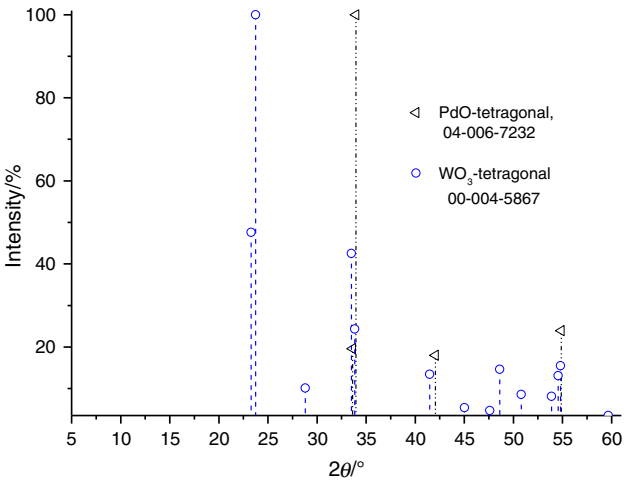

Fig. 6 X-ray diffraction lines for the main planes of reflections from Cs_3PW, WO_3 and PdO according to 00-050-1857 files

same two peaks of pure and Pd-doped HPCs. Thus, the height of the peak at $2\theta = 33.506$ ($I_{111} = 42.5$) was divided by the height of the peak at $2\theta = 23.754$ ($I_{110} = 100$), which is the characteristic of WO_3. The ratio I_{111}/I_{110} from spectra corresponding to heated samples at 873 K for HPCs containing Pd is higher than for undoped HPCs, because the intensity for the peak at $2\theta = 33.506$ was increased owing to superposition of the peak at $2\theta = 33.855$ ($I_{101} = 100$) belonging to PdO [17]. This is a proof of PdO formation at thermal decomposition of Pd-doped HPCs.

Thermal analysis

The thermal curves of decomposition for all synthesized compounds and all heating rates, without the isothermal segments at 573 K, can be seen in Figs. 7 and 8.

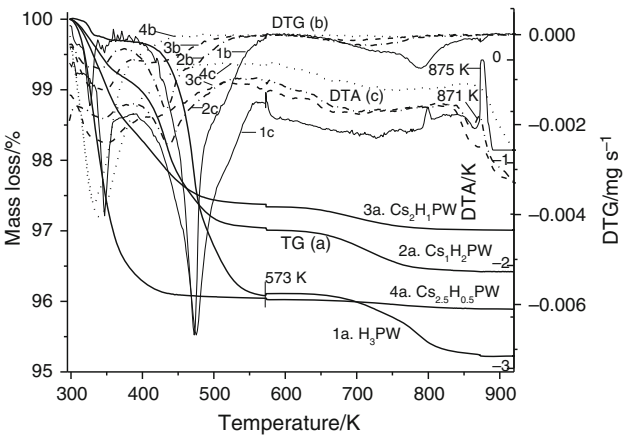

Fig. 7 The thermal curves of decomposition for H_3PW and $Cs_xH_{3-x}PW$, where $x = 1$, 2 and 2.5: TG (*1a–4a*), DTG (*1b–4b*) and DTA (*1c–4c*)

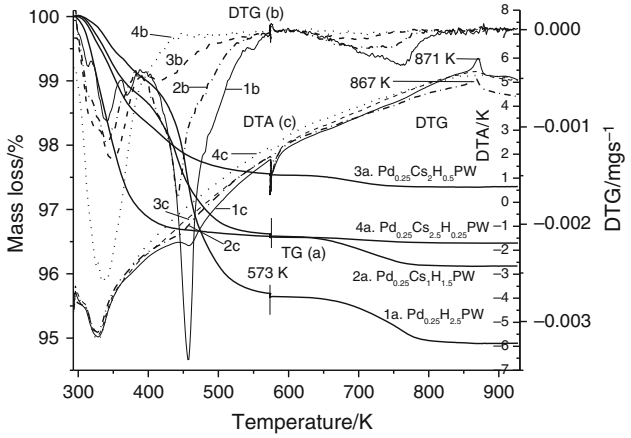

Fig. 8 The thermal curves of decomposition for $PdH_{2.5}PW$ and $PdCs_xH_{2.5-x}PW$, where $x = 1$, 2 and 2.5: TG (*1a–4a*), DTG (*1b–4b*) and DTA (*1c–4c*)

The thermal decomposition of the $H_3PW{\cdot}xH_2O$ and its acid Cs salts occurs between 298 K and about 900 K. The final decomposition temperature depends on the composition and the used heating rate. Thus, the thermal analysis of the $H_3PW{\cdot}xH_2O$ shows the loss of water in three steps. The first one corresponds to the loss of the physically adsorbed water and the water molecule bound by weak hydrogen bonds (about 6–8 H_2O molecules/KU) in the temperature range of 298–383 K. The second step corresponds to the water molecules from $H_5O_2^+$ expelled in the range of 383–573 K corresponding to $H_3PW{\cdot}6H_2O$ dehydration. The third step is the constitutional water loss, over 573 K [the water formed of the protons and the oxygen of the $[PW_{12}O_{40}]^{3-}$]. The water molecules bound by weak hydrogen bonds and the water molecules of $H_5O_2^+$ are considered as crystallization water. The TG–DTA experiments have shown the complete elimination of the physically adsorbed water and the crystallization water from $H_3PW{\cdot}xH_2O$ after isothermal heating at 573 K for 1 h (this segment of isothermal heating is not shown in Figs. 7, 8).

The decomposition of $Cs_1H_2PW{\cdot}5H_2O$ and $Cs_2HPW{\cdot}5H_2O$ owing to the loss of water in three steps also can be observed on TG curves, and the maxima rates for these steps are evidenced on the DTG curves. In the $Cs_{2.5}H_{0.5}PW$ case, the second step (the water bonded as $H_5O_2^+$) could be observed just a shoulder on the DTG curve. The peak size corresponding to constitutive water loss on DTG curve is diminished strongly as result of Cs/KU ratio increasing, this means lower H^+/KU ratio. On the other hand, a high content of physically adsorbed water (probable water of pores, which is removed at lower temperature as the water molecules bond of H^+) was evidenced for the salts with higher specific surface area, $Cs_2HPW{\cdot}4–5H_2O$ and $Cs_{2.5}H_{0.5}PW{\cdot}6–8H_2O$ [16].

The final process of WO_3 crystallization gives exothermal peaks on DTA curves for H_3PW and Cs_1H_2PW, only shoulders for Cs_2HPW and shows no significant thermal effect for $Cs_{2.5}H_{0.5}PW$.

Generally, the thermal decomposition of Pd-doped HPCs occurs in the same manner, but at lower temperature than corresponding undoped HPCs as it ensues from thermal curves showed in Fig. 8.

On the other hand, the acidic salts can be written down as mixture of H_3PW and Cs_3PW, thus: $6Cs_{2.5}H_{0.5}PW = 1H_3PW + 5Cs_3PW$, $3Cs_2HPW = 1H_3PW + 2Cs_3PW$, $3CsH_2PW = 2H_3PW + 1Cs_3PW$ and as general formula: $Cs_xH_{3-x}PW \cdot yH_2O = (1 - x/3)H_3PW + Cs_x[PW]_{x/3}$ [16]. The Pd-doped $Cs_xH_{3-x}PW \cdot yH_2O$ is a mixture of H_3PW, Cs_3PW and PdHPW based on the experimental data, and their composition could be described by general formula: $6Pd_{0.25}Cs_xH_{2.5-x}PW \cdot yH_2O = 1.5PdHPW + (4.5 - 2x)H_3PW + 2xCs_3PW$ [17].

All the experimental observations and previous assumptions lead to the conclusion that only the KUs belonging to H_3PW or PdHPW were decomposed to oxides as result of constitutive water release over 573 K.

The mass loss between 573 and 923 K gives very close values to the theoretical ones for the content of constitutive water for the prepared HPCs, excepting the $Pd_{0.25}Cs_xH_{2.5-x}PW$ for $x = 2.5$, which has to be a neutral salt according this general formula, but the calculation gives the $Pd_{0.25}Cs_{2.5}H_{0.25}PW$ formula.

Based on these observations and on the thermal analyses results, the main decomposition processes of $H_3PW{\cdot}xH_2O$ and $Cs_xH_{3-x}PW{\cdot}yH_2O$ and $Pd_{0.25}H_{2.5}PW{\cdot}6H_2O$ and $Pd_{0.25}Cs_xH_{2.5-x}PW{\cdot}yH_2O$ are described by the next relations:

$$H_3PW_{12}O_{40} \cdot xH_2O \xrightarrow[-xH_2O]{298-573\,K} H_3PW_{12}O_{40} \xrightarrow[-1/2H_2O]{573-923\,K} 12WO_3 + 1/2P_2O_5 \quad (1)$$

$$Cs_xH_{3-x}PW_{12}O_{40} \cdot yH_2O \xrightarrow[-yH_2O]{298-573\,K} (1 - x/3)H_3PW_{12}O_{40} + x/3Cs_3PW_{12}O_{40} \xrightarrow[-(3-x)/2H_2O]{573-923\,K} Cs_x(PW_{12}O_{40})_{x/3} + 12(1 - x/3)WO_3 + (1 - x/3/2)P_2O_5 \quad (2)$$

$$4Pd_{0.25}H_{2.5}PW_{12}O_{40} \cdot 6H_2O \xrightarrow[-6H_2O]{298-573\,K} PdH_{2.5}W_{12}O_{40} + 3H_3PW_{12}O_4 \xrightarrow[-5H_2O]{573-923\,K} PdO + 48WO_3 + 2P_2O_5 \quad (3)$$

$$6Pd_{0.25}Cs_xH_{2.5-x}PW_{12}O_{40} \cdot yH_2O \xrightarrow[-yH_2O]{298-573\,K} 1.5\,PdHPW_{12}O_{40} + (4.5 - 2x)H_3PW_{12}O_{40} + 2xCs_3PW_{12}O_{40} \xrightarrow[-3(2.5-x)H_2O]{573-923\,K} 1.5PdO + 2xCs_3PW_{12}O_{40} + 12(6 - 2x)WO_3 + 3P_2O_5 \quad (4)$$

The kinetics for constitutional water loss was studied using the Standard Test Method for Decomposition Kinetics by Thermogravimetry [2]. The segments of TG curves for nonisothermal heating from 573 to 923 K (see Fig. 9) were used to determine the absolute temperatures at constant conversion-α, for the range of constant conversion values from 5 to 20 %, with the interval of 5 %.

The activation energy was calculated with the next equation [2]:

$$E = -(R/b)\Delta(\log \beta)/\Delta\left(T^{-1}\right), \quad (5)$$

The symbols used have the following definitions:

R—gas constant, 8.314 Jmol^{-1} K^{-1}), b—approximation derivative, 0.457 for the first iteration, β—heating rate/K min^{-1}, T—temperature/K at constant conversion, $\Delta(\log \beta)/\Delta(T^{-1})$ = the slope of the Arrhenius plot for log β function of $1/T$ of constant conversion data.

According with this method, the calculation of E was repeated with the new value for b selected from the numerical integration constants table [2] function of the value for E/RT_c (T_c—temperature at constant conversion for the heating rate closest to the midpoint of the experimental heating rate, 5 K min^{-1} in our case) until the value for the activation energy changes by less 1 %. This last value is named refined activation energy—E_r.

The pre-exponential factor, A, was calculated with the Eq. (6):

$$A = -(\beta'/E_r)R\ln(1-\alpha)\,10^a, \quad (6)$$

The new symbols used have the following definitions:

β'—heating rate nearest the midpoint of the experimental heating rate, 5 K min^{-1}, E_r—refined activation energy, a—approximation integral from the numerical integration constants table [2].

The results of these calculations are showed in the Table 1.

The precision of the E_a calculation depends on the quality of the linear fit for the points of constant conversion with coordinates (T^{-1}, log β), as the slope ($\Delta(\log \beta)/\Delta(T^{-1})$) for their regression line is one of the factors in Eq. (5), so the correlation coefficient R^2 describes also the precision for the found E_r values.

Figure 10 shows a typical diagram used for calculation of the activation energy and pre-exponential factor by ASTM E 1641-04 method.

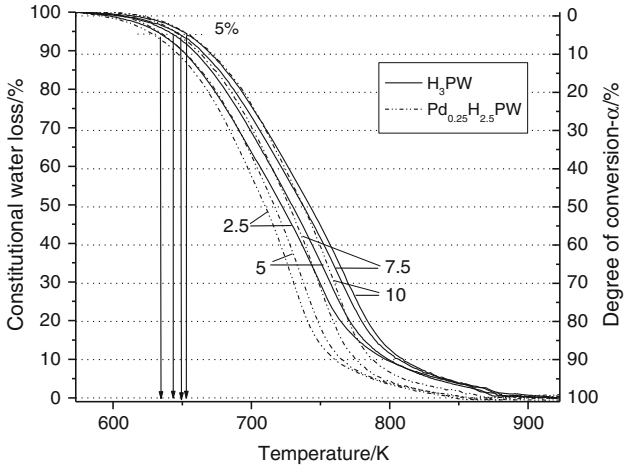

Fig. 9 The *curves* of constitutive water loss at the heating rate of 2.5, 5, 7.5 and 10 K min^{-1} for H_3PW and $Pd_{0.25}H_{2.5}PW$

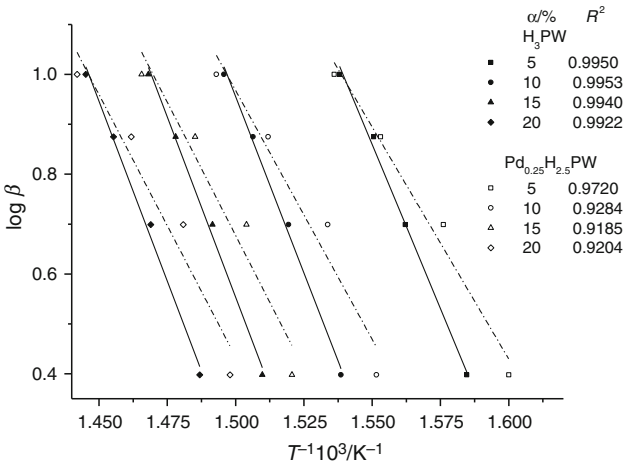

Fig. 10 The plot of log β versus inverse temperature (T^{-1}) at α = constant (5, 10, 15 and 20 %) for H_3PW and $Pd_{0.25}H_{2.5}PW$

Table 1 Apparent activation energy—E_a (kJ mol^{-1}) for H_3PW and $Cs_xH_{3-x}PW$, where x = 1, 2 and 2.5, calculated by ASTM E 1641-04 method (E_A) and by Friedman method (E_F)

α/%	H_3PW		Cs_1H_2PW		Cs_2H_1PW		$Cs_{2.5}$ $H_{0.5}PW$	
	E_A	E_F	E_A	E_F	E_A	E_F	E_A	E_F
5	241.5	258.1	267.0	284.2	200.8	239.0	188.8	161.9
10	259.4[1)]	266.3[2)]	258.7[3)]	265.3[4)]	247.5[5)]	258.5[6)]	199.7[7)]	189.1[8)]
15	265.1	274.7	255.9	272.8	247.2	260.7	216.8	191.5
20	264.6	268.9	265.9	281.7	263.8	279.8	224.1	189.4

Δ: [1)] ± 11.3, [2)] ± 19.3, [3)] ± 21.2, [4)] ± 20.2, [5)] ± 23.3, [6)] ± 8.7, [7)] ± 16.6, [8)] ± 7.0

The other way used for calculation of activation energy was the differential isoconversional method suggested by Friedman [5] based on the relation:

$$\ln(\beta\, d\alpha/dT) = \ln A + \ln(1-\alpha) - E_a(RT)^{-1}, \quad (7)$$

β—heating rate, K min^{-1}, A—pre-exponential factor, R—gas constant, 8.314 J mol^{-1} K^{-1}.

The plot of ln(β $d\alpha/dT$) vs. (T^{-1}), for α = constant and for a several heating rates, gives straight lines with the slope = E_a/R.

A typical figure for the E_a calculation by differential isoconversional method (Friedman) is showed in Fig. 11.

The apparent activation energies for constitutive water release from acidic HPCs by both methods (ASTM E 1641-04 and Friedman) are summarized in the Tables 1 and 2.

The imprecision in calculation of the apparent activation energy is related to the imprecision in the slope value determination: $\Delta(\log \beta)/\Delta(T^{-1})$ for the ASTM E 1641-04 method and E_a/R for Friedman method, and it was calculated on this basis. The limits of imprecision (Δ) are given under the Tables 1 and 2.

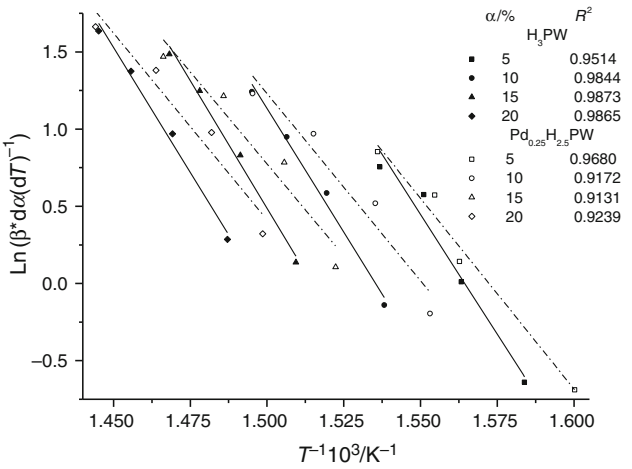

Fig. 11 The plot of ln (β*dα(dT)$^{-1}$) versus inverse temperature (T^{-1}) at α = constant (5, 10, 15 and 20 %) for H_3PW and $Pd_{0.25}H_{2.5}PW$

The differential format of data (dα/dT vs. T) produces high error bars in the energy plot, when it is accompanied of significant baseline noise, giving sharp variations on curves [30]. On the other hand, the application of curve-smoothing procedures may often influence the value of E_a [31]. However, good results were obtained choosing carefully the parameters of smoothing, without changing the base shape of curves, only for the samples with lower mass loss, where the influence of noise is important (Cs_2H_1PW, $Cs_{2.5}H_{0.5}PW$, $Pd_{0.25}Cs_2H_{0.5}PW$ and $Pd_{0.25}Cs_{2.5}H_{0.25}PW$).

The E_a values for the H_3PW and Cs_1H_2PW from Table 1 are very close because the Cs_1H_2PW's microstructure consists of mixture with ratio = 2:1 between the H_3PW and the Cs_3PW, with a core of Cs_3PW crystallites covered of H_3PW molecules as outer layers [16] having similar secondary structure with the H_3PW in bulk as it appears from their X-ray diffraction spectra. The Pd doping causes a drastic decrease of E_a because it supports the release of constitutional water by replacing of protons (see Table 2).

The thermal lifetime calculation has regard to the procedure stipulated of Standard Practice for Calculating Thermal Endurance of Materials from Thermogravimetric Data [22] based on the work of Krizanovsky and Mentlik [32]. The Eq. (8) was used to plot the logarithm of estimated thermal life (t_f) versus reciprocal of T_f:

$$\log t_f = E/(2.303\, RT_f) + \log[E/(R\beta)] - a \quad (8)$$

t_f—estimated thermal life for a given value of α/min, T_f—failure temperature for a give value of α/K, a—approximation integral taken from Table 1, ASTM E 1877-00.

To calculate t_f, the value for the temperature at the constant conversion point (T_c) for a heating rate (β) nearest the midpoint of the experimental heating rates was selected.

This value, along with the Arrhenius activation energy, was used to calculate the quantity $E/(R\,T_c)$ and to select the "a" value in Table 1 [22]. A number of temperatures in the region of the chosen percent mass loss, indicative of failure, were arbitrarily selected, in the mass change curve at the midpoint of heating rate. The logarithm of the thermal

Table 2 Apparent activation energy—E_a (Kj/mol) for $Pd_{0.25}H_{2.5}PW$ and $Pd_{0.25}Cs_xH_{2.5-x}PW$, where x = 1,2 and 2.5, calculated by ASTM E 1641-04 method (E_A) and by Friedman method (E_F)

α/%	$Pd_{0.25}H_{2.5}PW$		$Pd_{0.25}Cs_1H_{1.5}PW$		$Pd_{0.25}Cs_2H_{0.5}PW$		$Pd_{0.25}Cs_{2.5}H_{0.25}PW$	
	E_A	E_F	E_A	E_F	E_A	E_F	E_A	E_F
5	163.5	205.4	187.1	221.7	159.3	237.8	172.4	97.2
10	175.4[1)]	201.7[2)]	208.5[3)]	213.5[4)]	174.1[5)]	205.8[6)]	185.6[7)]	197.1[8)]
15	189.0	198.1	210.1	221.5	184.9	212.1	180.9	205.4
20	186.1	201.2	216.9	235.1	199.2	226.0	187.8	236.0

Δ: [1)] ± 15.8, [2)] ± 17.1, [3)] ± 20.1, [4)] ± 20.7, [5)] ± 16.7, [6)] ± 12.5, [7)] ± 2.0, [8)] ± 6.2

life from Eq. (4) was calculated. Finally, the thermal endurance curves were plotted, with thermal life on the ordinate and reciprocal of absolute temperature on the abscissa as can be seen in Figs. 12–15.

The failure temperature was chosen for $\alpha = 10$ % from two main reasons:

- It represents an important loss of active sites (10 %), which in many cases requires the replacement of catalyst; therefore it could be close to a practical application.
- The apparent activation energy at 10 % conversion is within the range of recommended conversion for the use of ASTM E 1641-04 method, because the value of the calculated activation energy is independent of reaction order only in the early stages of decomposition.

It is worthy to mention that the experimental temperature range (573–923 K) is close to the temperature range of predictions (523–623 K), according to the recommendations stipulated by ICTAC Kinetics Committee [33].

The significant lifetimes of HPCs are obtained for temperatures below 573 K. The lifetime with suitable length for use in practice could be fulfilled of the H_3PW and $Cs_xH_{3-x}PW$, where $x = 1$, 2 and 2.5, and only in certain cases of Pd-doped H_3PW and $Cs_xH_{3-x}PW$, where $x = 1$, 2 and 2.5.

The checking of lifetime prediction was carried out comparing the conversions obtained by heating the samples of H_3PW and Pd-doped H_3PW at 623 K for the time given in Figs. 12–15, when the conversions of 10 % were reached. Their lifetimes determined using E_a either calculated with ASTM E 1641-04 or with Friedman method are very close. As consequence, values around 12 % conversions were obtained for both HPCs, but with a difference of 2 % by comparison with the conversion of 10 % expected

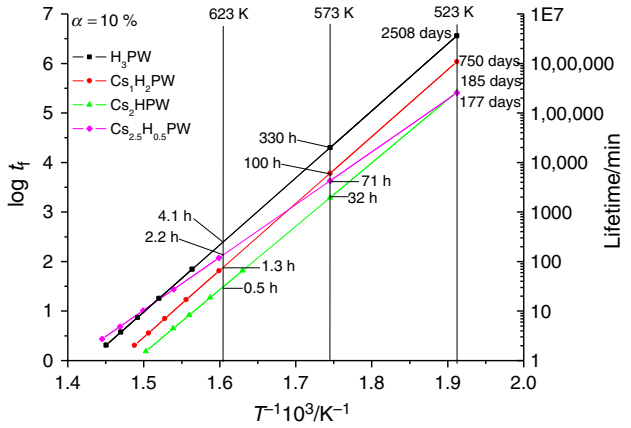

Fig. 12 The decimal logarithm of the lifetime and lifetime (calculated with E_a from Table 1) calculated versus reciprocal temperature for the H_3PW and some of its acidic Cs salts at $\alpha = 10$ %

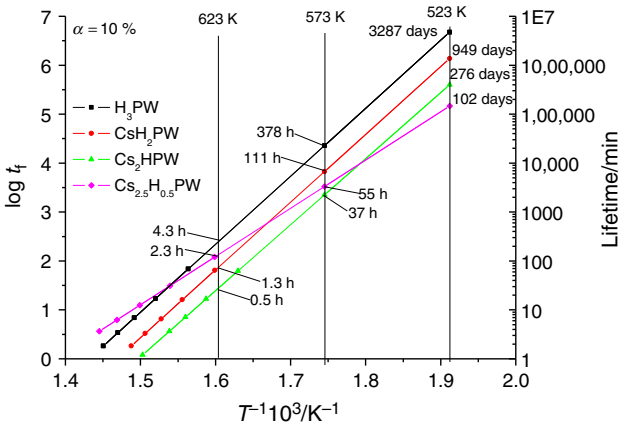

Fig. 14 The decimal logarithm of the lifetime and lifetime (calculated with E_a from Table 2) calculated vs reciprocal temperature for the H_3PW and some of its acidic Cs salts at $\alpha = 10$ %

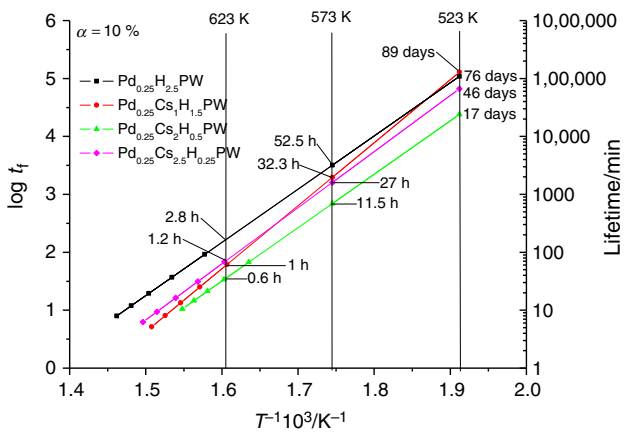

Fig. 13 The decimal logarithm of the lifetime and lifetime (calculated with E_a from Table 1) versus reciprocal temperature for the Pd-doped H_3PW and some of its acidic Cs salts at $\alpha = 10$ %

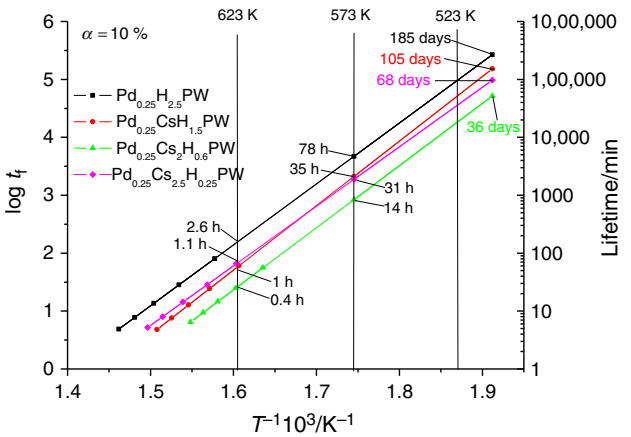

Fig. 15 The decimal logarithm of the lifetime and lifetime (calculated with E_a from Table 2) versus reciprocal temperature for the Pd-doped H_3PW and some of its acidic Cs salts at $\alpha = 10$ %

Table 3 The limits of catalysts' lifetime calculated on the basis of the imprecision in determination of apparent activation energy (Δ) with ASTM1641-04 method—E_A and Friedman method—E_F

Catalysts	Temp./K	Limits of the t_f/h			
		E_A—ASTM 1641-04		E_F—Friedman	
		t_f ($E_A - \Delta$)	t_f ($E_A + \Delta$)	t_f ($E_F - \Delta$)	t_f ($E_F + \Delta$)
H_3PW	523	49,700.4	71,808.9	48,939.6	112,236.0
	573	299.7	363.9	260.8	510.8
Cs_1H_2PW	523	13,303.9	24,425.0	15,192.8	31,090.1
	573	86.9	116.6	82.1	143.4
Cs_2H_1PW	523	3413.0	6657.3	5191.9	8313.5
	573	28.7	38.3	34.5	42.5
$Cs_{2.5}$ $H_{0.5}PW$	523	3018.1	5922.2	1985.7	3215.3
	573	60.0	83.9	51.5	63.0
$Pd_{0.25}H_{2.5}PW$	523	1332.3	2689.0	3135.8	5943.2
	573	45.6	64.8	60.1	98.5
$Pd_{0.25}Cs_1H_{1.5}PW$	523	1490.1	3095.7	1718.0	3499.2
	573	27.9	38.7	27.6	44.7
$Pd_{0.25}Cs_2H_{0.5}PW$	523	290.1	548.8	674.0	1135.2
	573	10.5	12.9	12.0	16.5
$Pd_{0.25}Cs_{2.5}H_{0.25}PW$	523	1030.1	1171.9	1437.3	1817.6
	573	25.9	27.2	28.9	33.2

according to lifetime calculation. This result confirms satisfactorily the calculation of lifetime and implicitly the used values of apparent activation energy.

On the other hand, the imprecisions in determination of activation energies affected strongly the catalysts' lifetime prediction, because the limit values of apparent activation energies gave a large domain for the lifetimes, as you can see in Table 3. However, the same conclusions could be drawn based on these values for selection of suitable catalysts, as those deduced based on the lifetime calculated with the most probable activation energies.

Narrower limits of lifetime prediction need higher accuracy and precision in determination of apparent activation energy, which becomes increasingly easier with the new performant equipment and the new computational methods.

Conclusions

The thermal decomposition of H_3PW and some of its acidic Cs salts in pure form and as Pd-doped form consists of water release: physically adsorbed water, hydrogen-bonded water and constitutive water [the water formed of the protons and the oxygen of the $(PW_{12}O_{40})^{3-}$]. The constitutive water loss occurs with significant rate over 573 K. The release of constitutive water causes the destroying of Keggin units with formation of corresponding oxides and the loss of acidic catalytic activity. The apparent activation energy—E_a for constitutive water release was determined by integral isoconversional method—ASTM 1641-04 and differential isoconversional method—Friedman. The thermal endurance was estimated by comparing the E_a for studied HPCs and mainly by their lifetime calculated according to the Standard Practice for Calculating Thermal Endurance of Materials from Thermogravimetric Data (ASTM E 1877-00) with the most reliable E_a values.

The Pd-doped HPCs show significantly lower values of E_a than pure HPCs. Generally, the E_a calculated by Friedman differential method are bigger than those calculated with FW-ASTM 1641-04, except E_a value for $Cs_{2.5}$ $H_{0.5}PW$. Between the E_a values calculated by the two methods, the greatest differences are observed for $\alpha = 5$ and 20 %. On this basis and the assumption from ASTM 1641-04 that the value of activation energy is independent of reaction order only in the early stages of decomposition, the E_a values for $\alpha = 10$ % were used for calculation of lifetime. The explanation could be the significant error of mass loss measurement at low conversion (for $\alpha \leq 5$ %) and deviation from the assumption that E_a is independent of reaction order in the early stages of decomposition, id est when $\alpha > 15$ %.

The significant lifetimes of HPCs are obtained for temperatures below 573 K, but lifetime with suitable length for use in practice could be fulfilled of the H_3PW and $Cs_xH_{3-x}PW$, where $x = 1$, 2 and 2.5, and only in certain cases of Pd-doped H_3PW and Pd-doped $Cs_xH_{3-x}PW$, where $x = 1$, 2 and 2.5.

The checking of lifetime prediction was carried out comparing the conversions obtained by heating the samples of H_3PW and Pd-doped H_3PW at 623 K for the time at which the conversions of 10 % have to be reached according to the calculations. The values around 12 % conversion obtained for both HPCs confirm satisfactorily the calculation of lifetime and implicitly the used values of apparent activation energy.

Acknowledgements The authors gratefully acknowledge the financial support of HURO/0901/090/2.2.2 project, Hungary-Romania Cross Border Cooperation Programme 2007–2013 and Romanian Academy-Institute of Chemistry Timisoara-Research Programme no. 4.

References

1. Criado JM, Sánchez-Jiménez PE, Pérez-Maqueda LA. Critical study of the isoconversional methods of kinetic analysis. J Therm Anal Calorim. 2008;92:199–203.
2. ASTM E 1641-04. Standard test method for decomposition kinetics by thermogravimetry. 2004. doi:10.1520/E1641-04.
3. Flynn JH, Wall LA. A quick direct method for the determination of activation energy from thermogravimetric data. Polym Lett. 1966;4:323–8.
4. Flynn JH. The isoconversional method for determination of energy of activation at constant heating rates. J Therm Anal. 1983;27:95–102.
5. Friedman HL. Kinetics of thermal degradation of char-forming plastics from thermogravimetry application to a phenolic plastic. J Polym Sci. 2007;6:183–95.
6. Budrugeac P. Differential non-linear isoconversional procedure for evaluating the activation energy of non-isothermal reactions. J Therm Anal Calorim. 2002;68:131–9.
7. Mizuno N, Misono M. Heterogeneous catalysis. Chem Rev. 1998;98:199–217.
8. Cavani F. Heteropolycompound-based catalysts: a blend of acid an oxidizing properties. Catal Today. 1998;41:73–86.
9. Okuhara T, Mizuno N, Misono M. Catalysis by heteropoly compounds-recent developments. Appl Catal A: Gen. 2001;222:63–77.
10. Shanbhag GV, Bordoloi A, Sahoo S, Devassy BM, Halligudi SB. Environmentally benign catalysts: for clean organic reactions. Berlin: Springer; 2013.
11. Narasimharao K, Brown DR, Lee AF, Newman AD, Siril PF, Tavener SJ, Wilson K. Structure-activity relations in Cs-doped heteropolyacid catalysts for biodiesel production. J Catal. 2007;248:226–34.
12. Siddqui MRH, Holmes S, He H, Smith W, Coker EN, Atkins MP, Kozhevnikov IV. Coking and regeneration of palladium-doped $H_3PW_{12}O_{40}/SiO_2$ catalysts. Catal Lett. 2000;66:53–7.
13. Palcheva R, Spojakina A, Tyuliev G, Jiratova K, Petrov L. Thiophene hydrodesulfurization activity of alumina supported heteropoly compounds: nickel effect. React Kinet Catal Lett. 2006;89:285–92.
14. Volkova GG, Plyasova LM, Salanov AN, Kustova GN, Yurieva TM, Likholobov VA. Heterogeneous catalysts for halide-free carbonylation of dimethyl ether. Catal Lett. 2002;80:175–9.
15. Aouissi A, Al-Deyab SS, Al-Owais A, Al-Amro A. Reactivity of heteropolytungstate and heteropolymolybdate metal transition salts in the synthesis of dimethyl carbonate from methanol and CO_2. Int J Mol Sci. 2010;11:2770–9.
16. Sasca VZ, Verdes O, Avram L, Popa A, Erdöhelyi A, Oszko A. The $Cs_xH_{3-x}PW_{12}O_{40}$ catalysts microstructure model. Appl Catal A: Gen. 2013;451:50–7.
17. Sasca VZ, Verdeş O, Avram L, Popa A. Thermal decomposition of Pd doped 12-tungstophosphoric acid and some of its cesium salts. Rev Roum Chim. 2013;58:451–61.
18. Kozhevnikov IV. Heterogeneous acid catalysis by heteropoly acids: approaches to catalyst deactivation. J Mol Catal A. 2009;305:104–11.
19. Guisnet M, Magnoux P. Organic chemistry of coke formation. Appl Catal A: Gen. 2001;212:83–96.
20. Kozhevnikov IV. Sustainable heterogeneous acid catalysis by heteropoly acids. J Mol Catal A. 2007;262:86–92.
21. Wang B, Manos G. A novel thermogravimetric method for coke precursor characterisation. J Catal. 2007;250:121–7.
22. ASTM E 1877-00 (Reapproved 2005). Standard practice for calculating thermal endurance of materials from thermogravimetric data.
23. Misono M, Mizuno N, Katamura K, Kasai A, Konishi Y, Sakata K, Okuhara T, Yoneda Y. Catalysis by heteropoly compounds: the structure and properties of 12-heteropolyacids of molybdenum and tungsten ($H_3PMo_{12-x}W_xO_{40}$) and their salts pertinent to heterogeneous catalysis. Bul Chem Soc Jpn. 1982;55:400–6.
24. Rocchiccioli-Deltcheff C, Fournier M, Franck R, Thouvenot R. Vibrational investigations of polyoxometalates. 2: evidence for anion-anion interactions in molybdenum(VI) and tungsten(VI) compounds related to the Keggin structure. Inorg Chem. 1983;22:207–16.
25. Essayem N, Holmqvist A, Gayraud PY, Vedrine JC, Taarit YB. In situ FTIR studies of the protonic sites of $H_3PW_{12}O_{40}$ and its acidic cesium salts $M_xH_{3-x}PW_{12}O_{40}$. J Catal. 2001;197:273–80.
26. Highfield JG, Moffat JB. Characterization of 12-tungstophosphoric acid and related salts using photoacoustic spectroscopy in the infrared region. I: thermal stability and interactions with ammonia. J Catal. 1984;88:177–87.
27. Brown GM, Noe-Spirlet MR, Busing WA, Levy HA. Dodecatungstophosphoric acid hexahydrate, $(H_5O_2^+)_3(PW_{12}O_{40}^{3-})$: the true structure of Keggin's 'pentahydrate' from single-crystal X-ray and neutron diffraction data. Acta Cryst B. 1977;33:1038–46.
28. Okumura K, Yamashita K, Yamada K, Niwa M. Studies on the identification of the heteropoly acid generated in the H_3PO_4–WO_3–Nb_2O_5 catalyst and its thermal transformation process. J Catal. 2007;245:75–83.
29. Yang H, Shang F, Gao L, Han H. Structure, electrochromic and optical properties of WO_3 film prepared by dip coating-pyrolysis. Appl Surf Sci. 2007;253:5553–7.
30. Zhang X, He C, Wang L, Li Z, Feng Q. Synthesis, characterization and nonisothermal decomposition kinetics of $La_2(CO_3)_3$-$3.4H_2O$. J Therm Anal Calorim. 2015;119:1713–22.
31. Neglur R, Grooff D, Hosten E, Aucamp M, Liebenberg W. Approximation-based integral versus differential isoconversional approaches to the evaluation of kinetic parameters from thermogravimetry. J Therm Anal Calorim. 2016;123:2599–610.
32. Krizanovsky L, Mentlik V. The use of thermal analysis to predict the thermal life of organic electrical insulating materials. J Therm Anal. 1978;13:571–8.
33. Vyazovkin S, Burnham AK, Criado JM, Pérez-Maqueda LA, Popescu C, Sbirrazzuoli N. ICTAC kinetics committee recommendations for performing kinetic computations on thermal analysis data. Thermochim Acta. 2011;520(1–2):1–19.